

Anisotropic order-disorder vortex transition in $\text{La}_{2-x}\text{Sr}_x\text{CuO}_4$

Y. Radzyner, A. Shaulov, and Y. Yeshurun

Department of Physics, Institute of Superconductivity, Bar-Ilan University, Ramat-Gan 52900, Israel

I. Felner

Racah Institute of Physics, The Hebrew University, Jerusalem 91904, Israel

K. Kishio and J. Shimoyama

Department of Applied Chemistry, The University of Tokyo, Tokyo 113-8656, Japan

(Received 30 October 2001; revised manuscript received 4 March 2002; published 7 June 2002)

We report on magnetization measurements in $(\text{La}_{0.937}\text{Sr}_{0.063})_2\text{CuO}_4$ crystals with the field either parallel or perpendicular to the c axis. A second magnetization peak (“fishtail”), interpreted as indicating a vortex order-disorder transition, is observed in both directions. Differences in the details of the fishtail anomaly in the two directions (width, temperature and time dependence, and history effects) are attributed to the anisotropy and the twin boundaries in the ab plane. The transition fields in both directions, although different in magnitude, exhibit similar qualitative behavior, namely, a strong decrease with temperature in the entire measured range. This unique behavior is explained postulating that *both* thermally and disordered induced fluctuations contribute to the destruction of the vortex lattice. The resulting “pinned liquid” disordered state is characterized by large thermal fluctuations and irreversible magnetic behavior.

DOI: 10.1103/PhysRevB.65.214525

PACS number(s): 74.72.Dn, 74.60.Ge

I. INTRODUCTION

The nature of the various vortex matter phases in high-temperature superconductors (HTS's), and the transitions between them, have been the topic of many experimental and theoretical investigations.^{1–9} Two vortex order-disorder phase transitions have been identified: a melting transition into a liquid vortex state manifested by a discontinuous jump in the reversible magnetization,¹ and a solid-solid transition into an entangled vortex state³ manifested by the appearance of a second magnetization peak.

The magnetic phase diagram of anisotropic superconductors depends not only on the field and temperature, but also on the angle between the field and the c axis.^{10–12} Many experiments^{13–17} have verified that the standard scaling rules^{10,11} apply for the melting transition and for the irreversibility line¹⁸ in $\text{YBa}_2\text{Cu}_3\text{O}_{7-\delta}$ crystals. In the more anisotropic case of $\text{Bi}_2\text{Sr}_2\text{CaCu}_2\text{O}_{8+\delta}$ the scaling relation was shown to be invalid.^{19,20} Reports for the solid-solid transition, which is manifested by a fishtail, are mixed. Some reports²¹ verified that the scaling relation holds, while others^{20,22} needed to invoke a new scaling relation.

In this paper we present a study of the vortex order-disorder transition in $(\text{La}_{0.937}\text{Sr}_{0.063})_2\text{CuO}_4$, a HTS crystal with intermediate anisotropy $\varepsilon \approx 1/10 - 1/30$.^{6,23} The relatively large $(\text{La}_{0.937}\text{Sr}_{0.063})_2\text{CuO}_4$ crystals present a unique opportunity to study the order-disorder transition for both $H||c$ and $H||ab$, using the same crystal. Although some of the results for $H||ab$ were already presented in Ref. 24, for the purpose of comparison we present these data here in more detail, comparing details of the “fishtail” anomaly, i.e., temperature dependence, time dependence, and history effects, in both directions. We find differences in the magnitude of the transition fields in the two directions that cannot be explained by the standard scaling rules. These deviations

are attributed to either discretization owing to the layered structure of $\text{La}_{2-x}\text{Sr}_x\text{CuO}_4$ or to anisotropic pinning caused by twin boundaries.

II. EXPERIMENT

A single crystal of $(\text{La}_{0.937}\text{Sr}_{0.063})_2\text{CuO}_4$ was prepared by the traveling-solvent—floating-zone method.²⁵ Several samples were cut from this crystal, which has a critical temperature of about 32 K. Data will be shown for two samples denoted here as L1 and L2 with dimensions of $0.8 \times 2.5 \times 0.8$ and $0.35 \times 2.5 \times 0.8$ mm³, respectively. Sample L1 was chosen for its square cross section, which enables us to compare measurements, performed with the field parallel to the ab planes or perpendicular to them, avoiding corrections due to different geometries. In this sample we encountered problems in performing the history dependence measurements (Sec. V below). This was due to the relatively large field of full penetration (H^*), that masks history dependence effects, in the relatively thick L1 sample. To bypass this problem we took advantage of the different geometry of sample L2. This sample has a relatively low field of full penetration (H^*), enabling us a clear demonstration of history-dependent effects. We note that both samples give similar results in all other aspects. Measurements were performed using a commercial superconducting quantum interference device (SQUID) magnetometer (Quantum Design MPMS-5S). We present results obtained for a scan length of 4 cm. The main features of the fishtail and their temperature dependence were confirmed in an upgraded version of this SQUID, utilizing the RSO technique with 1-cm scans. Samples were glued on a fiberglass mount, which does not allow for deflection of the crystal during the measurement, despite the large forces acting on it. Samples were oriented with a possible deviation of a few degrees between measurements.

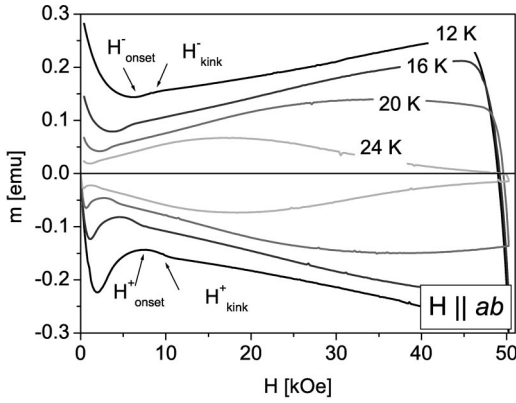


FIG. 1. Magnetization loops with the field parallel to the ab planes, at 12, 16, 20, and 24 K. Arrows point to four characteristic features of the loop.

III. ORDER-DISORDER TRANSITION LINE

The second magnetization peak ('fishtail') observed in a wide variety of HTS's such as $\text{Bi}_2\text{Sr}_2\text{CaCu}_2\text{O}_{8+\delta}$ (BSCCO),² $\text{Nd}_{1.85}\text{Ce}_{0.15}\text{CuO}_{4-\delta}$,³ untwinned $\text{YBa}_2\text{Cu}_3\text{O}_{7-\delta}$ (YBCO),^{4,5,26} $\text{Bi}_{1.6}\text{Pb}_{0.4}\text{Sr}_2\text{CaCu}_2\text{O}_{8+\delta}$,²⁷ $\text{La}_{2-x}\text{Sr}_x\text{CuO}_4$ (LaSCO),²⁸ and low- T_c superconductors such as CeRu_2 (Ref. 29) and 2H-NbSe_2 ,³⁰ has been associated with a transition between two vortex solid phases. As recently suggested by both experimental^{1-3,5,26,31-33} and theoretical^{7-9,34} works, this transition is between the quasi-ordered (Bragg glass) phase at low fields and the highly disordered (vortex glass, or entangled) phase at high fields. Pronounced features—onset,^{2,3} kink,^{5,35} or peak⁴—were identified as signifying this vortex solid-solid phase transition.

In Sec. III A we describe magnetization measurements performed on sample L1, with the field directed either parallel or perpendicular to the ab planes. Both configurations display a pronounced fishtail. Significant differences in the details of the fishtail characteristics in the two directions are described and discussed below.

A. Field parallel to ab planes

Figure 1 presents several magnetization loops of sample L1 with the magnetic field parallel to the ab planes, measured with a field step of 200 Oe. The loops display a pronounced "fishtail" with an onset at H_{onset}^+ (marked by an arrow), from which the persistent current commences to rise steeply until it changes slope at H_{kink}^+ .^{5,35,36} On the decreasing branch, the onset and the kink appear at different fields, thereby yielding four distinct features:³⁷ H_{onset}^+ and H_{kink}^+ and their counterparts on the descending branch H_{onset}^- and H_{kink}^- . The temperature dependence of these features is depicted in Fig. 2. Also depicted in the figure is the irreversibility line that was extracted from magnetization vs temperature measurements. Note that all four lines, representing the characteristic features of the fishtail, exhibit a steep *concave* descent with the increase of temperature. In Sec. IV we identify the $H_{\text{kink}}^-(T)$ curve as signifying an order-disorder transition line.

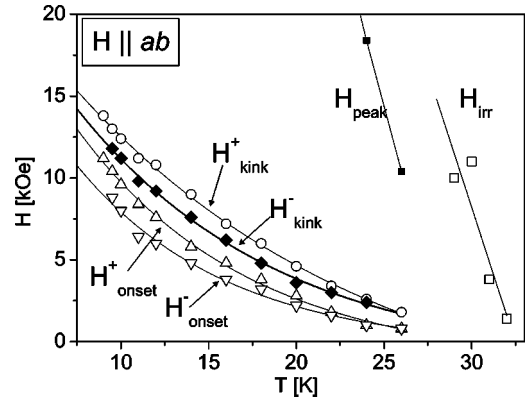


FIG. 2. Temperature dependence of H_{onset}^+ (up triangles), H_{kink}^+ (circles), H_{kink}^- (solid diamonds), H_{onset}^- (down triangles), H_{peak} (solid squares), and the irreversibility line (open squares) for $H||ab$. Lines are guides to the eye.

B. Field perpendicular to ab planes

The inset of Fig. 3 shows several magnetization loops, at different temperatures, measured in sample L1 with the magnetic field parallel to the c axis. The loops display a fishtail with a sharp onset (marked by an arrow). A kink, however, could not be detected, probably because of the presence of twin boundaries [a similar observation was made in YBCO where a kink is present in untwinned YBCO (Ref. 5) and absent in twinned YBCO (Ref. 38)]. The main panel of Fig. 3 shows the temperature dependence of the onset (both on the way up and on the way down), the peak (on both branches) and the irreversibility line. All these lines reveal a strong temperature dependence throughout the whole temperature range, similar to that observed with the field parallel to the ab planes. Corresponding features, appearing on the increasing and decreasing branches, occur at fields separated by roughly H^* , the field of full penetration.³⁹ Such a separation indicates that the two lines correspond to the same physical phenomenon, which would appear at the same in-

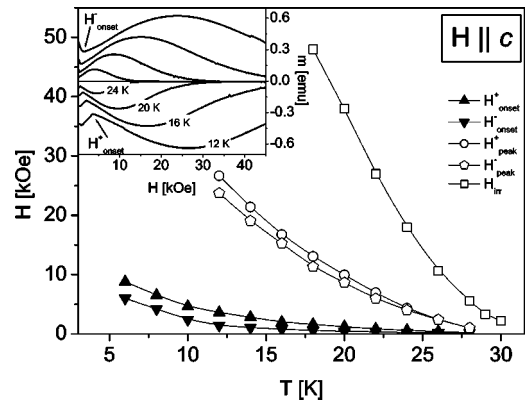


FIG. 3. Temperature dependence of the onset of an increasing branch (up triangles) and a decreasing branch (down triangles), the peak on the ascending branch (circles), the peak on the descending branch (hexagons), and the irreversibility line (open squares) $H||c$. Lines are guides to the eye. Inset: magnetization loops with the field parallel to the c axis, at 12, 16, 20, and 24 K. Arrows point to the onset fields.

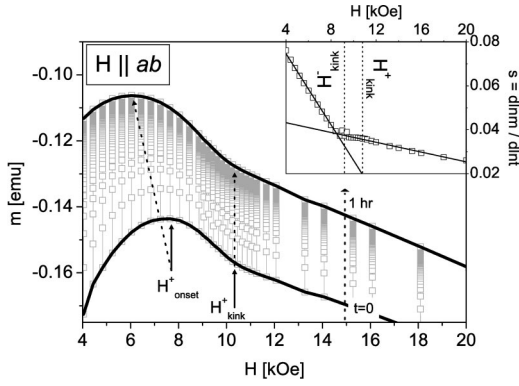


FIG. 4. Relaxation measurements at 12 K with $H||ab$, on the ascending branch of the loop. Gray columns represent measurements extended over an hour. Lines connect magnetizations at $t=0$ and $t=1$ h. Arrows point to the characteristic features. Note that H^+_{onset} shifts about 1 kOe, but H^+_{kink} is unaffected. Inset: dependence of the relaxation rate $s = d \ln m / d \ln t$ on field.

duction B . In global measurements such as this, the signal is integrated over the whole sample, resulting in a shift of H^* between the ascending and descending branches. Therefore, in the following we do not distinguish between corresponding features for this field direction.

In Sec. IV B we relate H_{onset} with the order-disorder phase transition for $H||c$. The similar qualitative behavior of the transition lines in the two directions suggests that the underlying physics of the transition is the same in both field directions.

IV. RELAXATION

Relaxation measurements were performed for both directions in an attempt to identify a change in the dynamics related to the vortex phase transition. These measurements were done on sample L1 utilizing the following protocol: Starting from a large negative field (where the field has penetrated fully), we have increased the field in steps of 200 Oe up to a field H . At this point, data was collected every minute for an hour. This process repeated for several fields H .

A. Field parallel to ab planes

Figure 4 depicts the time evolution of the magnetization in the ascending branch with $H||ab$ at 12 K. In this figure every column represents data collected for an hour. The solid lines in the figure connect values obtained at $t=1$ min and $t=1$ h. Note that the relaxation rate is quite large, between 15% and 20% in the course of an hour. Evidently, the position of the kink, H^+_{kink} , does not vary with time, while the onset field H^+_{onset} decreases appreciably over an hour. When performing the same procedure on the decreasing branch of the loop (not shown), the position of H^-_{kink} did not vary, while H^-_{onset} shifted to lower fields with time. These observations point to either of the kink fields, rather than the onset, as indicating an order-disorder transition, as previously found in YBCO.³⁷

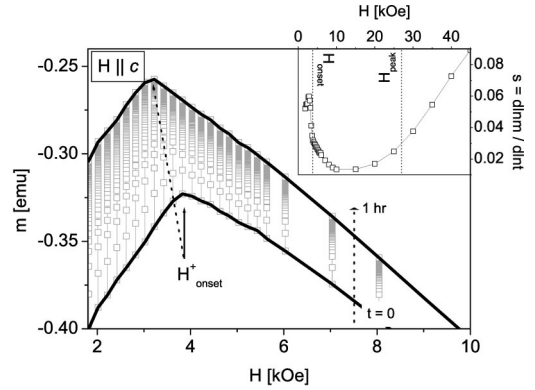


FIG. 5. Relaxation measurements at 12 K with $H||c$, on the ascending branch of the loop. Gray columns represent measurements extended over an hour. Lines connect magnetizations at $t=0$ and $t=1$ h. Arrows point to the characteristic features. Inset: dependence of the relaxation rate $s = d \ln m / d \ln t$ on field.

This result is further refined by measurements of the field dependence of the magnetic relaxation rate, $s = d \ln m / d \ln t$, as depicted in the inset to Fig. 4: Sharp changes in the slope of s vs field on *both* ascending and descending branches are observed at a field corresponding to H^-_{kink} , implying that this field signifies the vortex phase transition. The larger slope, at fields smaller than H^-_{kink} , corresponds to the quasi-ordered state, where the dominating elastic energy, E_{el} , is strongly dependent on field $E_{el} \sim B^{-1/2}$. The much weaker field dependence of the pinning energy, $E_{pin} \sim B^{-1/10}$, results in a weak field dependence of the relaxation rate at fields larger than H^-_{kink} .

B. Field perpendicular to ab planes

Figure 5 depicts the time evolution of the magnetization for $H||c$ at 12 K, using the same protocol and notations as Fig. 4. The onset fields, both on the way up and on the way down (not shown), shift to lower fields with time. The inset to Fig. 5 depicts the dependence of the relaxation rate s on field. The inset reveals a sharp change in the slope of $s(H)$ at a field located in close vicinity to H^+_{onset} . This sharp change in the slope of $s(H)$ —similar to that observed for $H||ab$ at the transition field—suggests that H^+_{onset} may be considered as indicating the vortex phase transition for $H||c$.

V. HISTORY DEPENDENCE

History dependence measurements around the phase transition line were performed in order to study the nature of the phase transition. For a first-order phase transition, near the phase transition line, supercooling and superheating effects may be observed.^{29,37,40} In this case, the magnetization of the sample may depend on its history, even after a field change larger than $2H^*$ (H^* is the Bean full penetration field³⁹). In order to detect such effects, we employed the “partial loop”^{29,37,40} technique which compares a complete loop to a partial loop, where the field increase culminates at an arbitrary field lower than the maximum field of the complete loop. According to the Bean model⁴¹ after a field change of

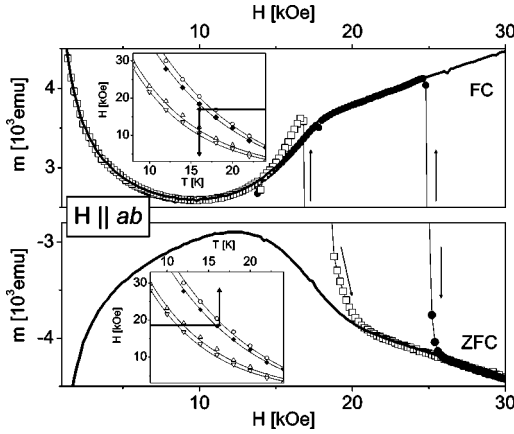


FIG. 6. Upper panel: descending branch of the complete magnetization loop at 16 K (solid line) and magnetization data after a field-cooling procedure with $H=25$ kOe (solid circles), and $H=17$ kOe (open squares). The inset describes the experimental procedure: cooling in field, then reducing field during measurement. Lower panel: ascending branch of the complete magnetization loop at 16 K (solid line) and magnetization data following a zero-field-cooling procedure with $H=25$ kOe (solid circles) and $H=18.6$ kOe (open squares). The inset describes the experimental procedure: zero-field cooling to 8 K with an increasing field, then warming up to a starting point and increasing field during measurement.

twice the profile depth, $2H^*$, all memory of previous conditions should be eradicated. For $H||ab$ we observe that when the maximum field of the partial loop is smaller than H_{onset}^- or larger than H_{kink}^+ , then after a field change larger than $2H^*$ all memory of previous conditions is erased, in accordance with the Bean model.⁴¹ However, if the ascent of the field is terminated in the region $H_{onset}^- < H < H_{kink}^+$ the descending branch of the partial loop may undershoot the descending branch of the complete loop.³⁷ Similarly, if the descent of the field is terminated in this region and the field commences to be raised, the magnetization may overshoot the lower (ascending) branch of the magnetization loop.³⁷

In the following we describe experiments obtained in sample L2. This sample is suitable for this type of experiments since for this thin sample the interval $H_{onset}^- < H < H_{kink}^+$ is much larger than $2H^* \approx 200$ Oe at 16 K.

A. Field parallel to ab planes

Two types of experiments—referred to as field cooling and zero-field cooling—were performed on sample L2. Field cooling experiments use the following procedure (see the inset to the top panel of Fig. 6): The sample is cooled from above T_c in a target field, and when a temperature of 16 K is reached the magnetization is measured while the field is lowered to zero in constant steps. We compare the magnetization curve thus obtained with the descending (upper) branch of the complete loop. As shown in the top panel of Fig. 6, when the target field is in the region $H_{onset}^- < H < H_{kink}^+$ the magnetization curve (open symbols) *overshoots* the complete loop (solid line). Curves generated from a target field outside

this region merge with the complete loop after a H^* change in field. Overshooting of the persistent current implies that a metastable disordered phase was “supercooled” to this region of the B - T phase diagram.

Zero-field-cooling experiments were performed using the following procedure (inset to bottom panel of Fig. 6): The sample is cooled in zero field to 8 K where the field is raised to a target value. At this field the sample is warmed to 16 K, and the magnetization is measured as the field is raised in constant steps. We compare the magnetization curve thus obtained with the ascending (lower) branch of the complete loop. The bottom panel of Fig. 6 shows that when the target field is in the region $H_{onset}^- < H < H_{kink}^+$ the resulting curve *undershoots* that of the complete loop, until it merges with the complete loop at H_{kink}^+ . When the target field is larger than H_{kink}^+ , the magnetization curve merges with the complete loop after a H^* change in field. Undershooting of the persistent current implies that a metastable ordered phase was “superheated” to this region of the B - T phase diagram.

The results of these experiments can be summarized as follows: (a) If the starting point of the measurement is in the range $H_{onset}^- < H < H_{kink}^+$, the measured magnetization does not overlap with the complete loop, despite having changed the field by more than $2H^*$. (b) The magnetization *overshoots* the complete loop if the starting point is reached via the disordered state. It *undershoots*, if the starting point is arrived at from the quasiordered state. (c) In all experiments, regardless of the history of the travel to the starting point, the curves merge with the complete loop at H_{kink}^+ for ascending fields and with H_{onset}^- for descending fields.

On the basis of the above experiments we conclude that the $H_{kink}^+(T)$ and $H_{onset}^-(T)$ lines determine the borders of the region where metastable states may exist. We now to discuss the physical meaning of the other two lines: $H_{onset}^+(T)$ and $H_{kink}^-(T)$. Recent experiments in BSCCO⁴² revealed that an abrupt change in the external field causes the injection of a transient disordered vortex state into the sample. This can be ascribed, for example, to surface imperfections and/or surface barriers, which impede the “smooth” entrance of the injected fluxons, as demonstrated by Paltiel *et al.* in NbSe₂.⁴³ When the thermodynamic conditions dictate a quasiordered state, the injected transient disordered state relaxes into a quasi-ordered state at a rate decreasing to zero as the induction approaches the transition line. Our procedures involve steps of 200 Oe between adjacent measurements. Thus generation of a transient disordered state can be expected after each step. Below H_{onset}^+ there is no change in the persistent current, implying that the lifetime of this transient state is much smaller than our time window and therefore a quasiordered state is measured. However, as H_{onset}^+ is approached, the lifetime of the transient disordered state is comparable to the time window of the measurement and therefore a larger persistent current is measured, indicating the existence of a disordered state. Reaching the higher limit for metastability, H_{kink}^+ , the disordered phase becomes the stable, thermodynamic phase.

We associate the remaining feature H_{kink}^- with the thermodynamic order-disorder phase transition. We base this iden-

tification on the relaxation measurements, which show that the relaxation rate changes dramatically at a field corresponding to H_{kink}^- , even on the ascending branch of the loop; see Sec. IV A. (We note that H_{kink}^- cannot be associated with the lifetime of the transient disordered state. This is because above the metastability region the thermodynamics dictate a disordered state, so that the phase introduced by the change of field does not alter the phase already existing in the sample.)

In view of the above, our results may be interpreted as follows: In the field-cooled experiment, a disordered state is dragged to below the transition line, H_{kink}^- , as evident from the overshoot of the magnetization curve. Therefore we have shown that the disordered phase may be supercooled to below the transition line. In the zero-field-cooled experiment, an ordered state is dragged to above the transition line, H_{kink}^- , as evident from the undershooting of the magnetization curve. Therefore we have shown that the disordered phase may be superheated to above the transition line. These observations are consistent with a first-order nature^{37,44} of the transition from quasiordered to disordered phases.

B. Field perpendicular to ab planes

Similar measurements performed with the $H||c$ in the region $H_{onset}^- < H < H_{onset}^+$ did not exhibit any history-dependent effects. The absence of such effects, as well as the absence of a kink in the magnetization loop, can be attributed to the smearing of the first-order nature of the transition by twin boundaries.⁴⁵

VI. SUMMARY AND DISCUSSION

The fishtail observed in the magnetization curves for both $H||ab$ and $H||c$ is similar to that observed in a wide variety of HTS crystals,²⁻⁵ and interpreted as signifying a vortex order-disorder phase transition. We propose a similar interpretation of the fishtails observed in LaSCO. Indeed, the similar qualitative behavior of the transition lines for $H||c$ and $H||ab$, (see Fig. 7), suggests that the underlying mechanism for these transitions is the same.

On the basis of the standard scaling relation^{10,46} one expects a ratio of $(1/\varepsilon) = 10-30$ (Refs. 6 and 23) between the transition fields for $H||c$ and $H||ab$. However, experimentally we measure a ratio of approximately 3; see Fig. 7. A possible reason for this large deviation may be based on the presence of twin boundaries, which contribute anisotropic pinning. On the other hand, one may not exclude the possibility that these large deviations from the scaling law indicate that the transitions for $H||ab$ and $H||c$ are of different nature, involving Josephson vortices in the former and Abrikosov vortices in the latter. Nevertheless, owing to the relatively small value of the anisotropy and the similar behavior of the transition for both directions, we tend to conclude that Abrikosov vortices rather than Josephson vortices, are involved.

One may attempt to interpret these transitions as driven by disorder-induced fluctuations, similar to the mechanism suggested for other HTS crystals.⁷⁻⁹ This implies a

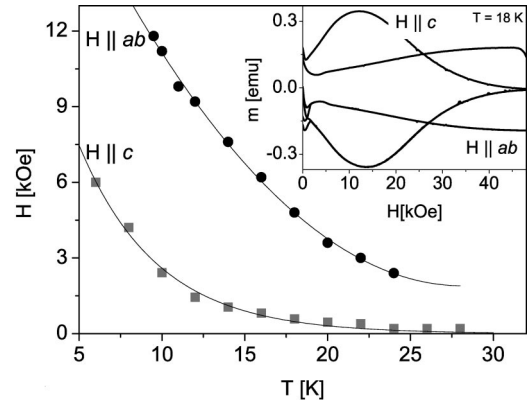


FIG. 7. Order-disorder transition lines in both $H||c$ (gray squares) and $H||ab$ (circles) configurations. Inset: magnetization loops for $H||c$ (gray) and $H||ab$ (black) at 18 K. The stronger pinning, in the $H||c$ configuration, influences both the width of the loop and the position of the transition line.

temperature-independent transition line at low temperatures.^{3,5} In LaSCO, however, in both $H||c$ and $H||ab$ the transition lines exhibit a strong decrease with temperature in the entire measured range.

An explanation based on the effects of surface barriers, which might obscure the features of the second peak anomaly at low temperatures,^{3,27,37,47} is excluded because of the fact that LaSCO the strong temperature dependence is common to the features measured on both ascending and descending branches. Another possible explanation may be associated with the influence of the persistent current: Strong currents may have a tendency to order the vortices,⁴⁸ so that the transition into a vortex glass would be deferred to higher fields. As temperature is decreased current increases, and its influence on the transition line should be marked. This explanation is precluded by the fact that the position of the kink is unaffected by the change in current; As can be seen from Fig. 4, within the time window of the measurement, the current relaxes to about 75% of its initial value, but the position of the kink is not altered, while within the same time window the onset field shifts by about 1 kOe.

As outlined in Ref. 49, we propose an explanation for the unique temperature dependence of the transition line measured in LaSCO, asserting that this transition is driven by *both* thermally- and disorder-induced fluctuations. The transition field is associated with the second magnetization peak, as is the solid-solid transition field, but depends strongly on temperature like the melting field. This strong temperature dependence implies that the transition to the disordered vortex state is driven not only by disorder-induced fluctuations, which are temperature independent far below T_c , but also by thermal fluctuations. As both thermal and disorder-induced fluctuations take a part in destabilizing the ordered solid, the interplay between *all three* energy scales E_{cl} , E_{pin} , and kT , should determine the transition line. The basic premise of our analysis is that an order-disorder transition occurs when the sum of thermal and disorder-induced displacements of the flux line, $\langle u_T^2 \rangle$ and $\langle u_{dis}^2 \rangle$ respectively, exceeds a certain fraction of the vortex lattice constant. A more accurate analysis should involve the averaged total displacement of the flux

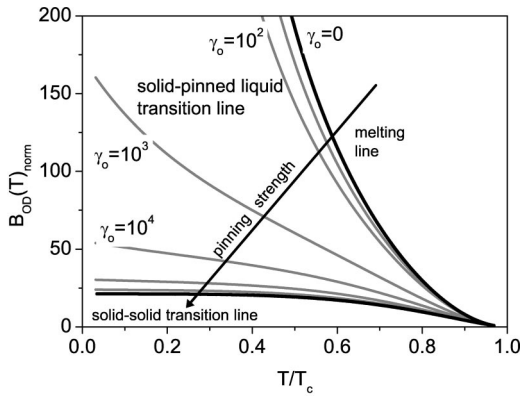


FIG. 8. Calculated transition lines assuming an order-disorder vortex phase transition driven by both thermally induced and disorder-induced fluctuations. The melting (entanglement) line is calculated by neglecting pinning (thermal) energy. All lines in between represent order-disorder transition lines in which both thermal and pinning energies are taken into account, but differ in the pinning strength.

line, which is not necessarily the sum of $\langle u_T^2 \rangle$ and $\langle u_{dis}^2 \rangle$. Yet, our simplified approach yields a qualitative description, and provides important insight.

The transition line $B_{OD}(T)$ can also be derived by considering the energy balance at the transition: $E_{el} = E_{pin} + kT$.^{24,49} The transition occurs when the sum of pinning energy and thermal energy exceeds the elastic energy barrier. Both approaches—adding fluctuations or energies—yield the same result for $B_{OD}(T)$. In Fig. 8 we present numerical results of the order-disorder transition line $B_{OD}(T)$ for a constant anisotropy and different pinning strength characterized by the parameter γ_o . The “pure” melting line in the figure is obtained by neglecting the pinning energy, so that $E_{el} = kT$, whereas the “pure” solid-solid transition line is obtained by neglecting the thermal energy, i.e., when $E_{el} = E_{pin}$. All lines in between represent order-disorder transition lines in which both thermal and pinning energies are taken into account. By tuning the pinning strength one may change the shape of the transition line and the character of the disordered phase.

For intermediate values of γ_o , the behavior of the transition line is qualitatively similar to that of a melting line, however, it represents a transition to a disordered state exhibiting irreversible magnetic behavior. One may refer to this disordered state as a “pinned liquid state.” Our experimental results for $B_{OD}(T)$ in LaSCO (see Fig. 7), clearly indicate

that this sample provides an example of a transition into a vortex pinned liquid state driven by both thermally and disorder induced fluctuations.

The above treatment is applicable for analyzing our results for $H||c$. The same approach may apply also for $H||ab$, assuming that Abrikosov vortices, rather than Josephson vortices, are involved. Also we assume pinning by point defects, neglecting the intrinsic pinning between the Cu-O layers.

This approach suggests that the melting, solid-solid, and solid to pinned-liquid vortex phase transitions are different manifestations of the same order-disorder thermodynamic first order transition, which, in general, is driven by *both* thermally- and disorder-induced fluctuations. This is in accordance with several recent works in BSCCO,^{50,51} claiming that the vortex melting line and solid-solid transition line are two manifestations of the same first-order transition. Our results show that the behavior of the transition line and the nature of the disordered state are determined by the relative contribution of the disorder-induced fluctuations. When this contribution is negligible (dominates), a transition to a liquid (solid) disordered state is obtained. When the contributions of both thermally and disorder-induced fluctuations are significant, a transition to a pinned liquid state is obtained. Thus, the observed transition line retains the shape of the melting transition, but the pinning suffices for the transition to be observed as a second peak, and not as a jump in magnetization. Our $(\text{La}_{0.937}\text{Sr}_{0.063})_2\text{CuO}_4$ crystal presents such an intermediate case—a “pinned liquid” state—exhibiting a transition line qualitatively similar to that of a melting line but which represents a transition to a state with irreversible magnetic characteristics.

ACKNOWLEDGMENTS

This manuscript is part of Y.R.’s Ph.D. thesis. An important contribution from T. Sasagawa is acknowledged. Continuous and helpful discussions with A. E. Koshelev, D. Giller, and Y. Wolfus are gratefully acknowledged. Important comments from E. Zeldov, V. Geshkenbein, T. Giamarchi, and A. A. Zhukov are acknowledged. Y.R. acknowledges financial support from the Mifal Hapayis—Michael Landau Foundation. Y. Y. acknowledges support from the U.S.-Israel Binational Science Foundation. A.S. and I.F. acknowledge support from the Israel Science Foundation. This research was supported by The Israel Science Foundation—Center of Excellence Program, and by the Heinrich Hertz Minerva Center for High Temperature Superconductivity.

¹E. Zeldov, D. Majer, M. Konczykowski, V. B. Geshkenbein, V. M. Vinokur, and H. Shtrikman, *Nature (London)* **375**, 373 (1995).

²B. Khaykovich, E. Zeldov, D. Majer, T. W. Li, P. H. Kes, and M. Konczykowski, *Phys. Rev. Lett.* **76**, 2555 (1996).

³D. Giller, A. Shaulov, R. Prozorov, Y. Abulafia, Y. Wolfus, L. Burlachkov, Y. Yeshurun, E. Zeldov, V. M. Vinokur, J. L. Peng, and R. L. Greene, *Phys. Rev. Lett.* **79**, 2542 (1997).

⁴K. Deligiannis, P. A. J. de Groot, M. Oussena, S. Pinfeld, R. Langan, R. Gagnon, and L. Taillefer, *Phys. Rev. Lett.* **79**, 2121 (1997).

⁵D. Giller, A. Shaulov, Y. Yeshurun, and J. Giapintzakis, *Phys. Rev. B* **60**, 106 (1999).

⁶T. Sasagawa, K. Kishio, Y. Togawa, J. Shimoyama, and K. Kitazawa, *Phys. Rev. Lett.* **80**, 4297 (1998).

⁷T. Giamarchi and P. Le Doussal, *Phys. Rev. B* **55**, 6577 (1997).

- ⁸D. Ertas and D. R. Nelson, *Physica C* **272**, 79 (1996).
- ⁹V. Vinokur, B. Khaykovich, E. Zeldov, M. Konczykowski, R. A. Doyle, and P. H. Kes, *Physica C* **295**, 209 (1998).
- ¹⁰V. M. Vinokur, V. B. Geshkenbein, M. V. Feigel'man, and G. Blatter, *Phys. Rev. Lett.* **71**, 1242 (1993).
- ¹¹G. Blatter, M. V. Feigelman, V. B. Geshkenbein, A. I. Larkin, and V. M. Vinokur, *Rev. Mod. Phys.* **66**, 1125 (1994).
- ¹²A. E. Koshelev, *Phys. Rev. Lett.* **83**, 187 (1999).
- ¹³T. Ishida, K. Okuda, A. I. Rykov, S. Tajima, and I. Terasaki, *Phys. Rev. B* **58**, 5222 (1998).
- ¹⁴W. K. Kwok, S. Fleshler, U. Welp, V. M. Vinokur, J. Downey, G. W. Crabtree, and M. M. Miller, *Phys. Rev. Lett.* **69**, 3370 (1992).
- ¹⁵R. G. Beck, D. E. Farrell, J. P. Rice, D. M. Ginsberg, and V. G. Kogan, *Phys. Rev. Lett.* **68**, 1594 (1992).
- ¹⁶A. Schilling, R. A. Fisher, N. E. Phillips, U. Welp, W. K. Kwok, and G. W. Crabtree, *Phys. Rev. B* **58**, 11 157 (1998).
- ¹⁷A. Schilling, M. Willemin, C. Rossel, H. Keller, R. A. Fisher, N. E. Phillips, U. Welp, W. K. Kwok, R. J. Olsson, and G. W. Crabtree, *Phys. Rev. B* **61**, 3592 (2000).
- ¹⁸R. Prozorov, M. Konczykowski, B. Schmidt, Y. Yeshurun, A. Shaulov, C. Villard, and G. Koren, *Phys. Rev. B* **54**, 15 530 (1996).
- ¹⁹B. Schmidt, M. Konczykowski, N. Morozov, and E. Zeldov, *Phys. Rev. B* **55**, R8705 (1997).
- ²⁰S. Ooi, T. Shibauchi, N. Okuda, and T. Tamegai, *Phys. Rev. Lett.* **82**, 4308 (1999).
- ²¹C. M. Aegerter, J. Hofer, I. M. Savic, H. Keller, S. L. Lee, C. Ager, S. H. Lloyd, and E. M. Forgan, *Phys. Rev. B* **57**, 1253 (1998).
- ²²S. Ooi, T. Shibauchi, K. Itaka, N. Okuda, and T. Tamegai, *Phys. Rev. B* **63**, 020501 (2001).
- ²³N. E. Hussey, J. R. Cooper, R. A. Doyle, C. T. Lin, W. Y. Liang, D. C. Sinclair, G. Balakrishnan, D. M. Paul, and A. Revcolevschi, *Phys. Rev. B* **53**, 6752 (1996).
- ²⁴Y. Radzyner, A. Shaulov, Y. Yeshurun, I. Felner, K. Kishio, and J. Shimoyama, *Phys. Rev. B* **65**, 100503(R) (2002).
- ²⁵T. Kimura, K. Kishio, T. Kobayashi, Y. Nakayama, N. Motohira, K. Kitazawa, and K. Yamafuji, *Physica C* **192**, 247 (1992).
- ²⁶T. Nishizaki, T. Naito, and N. Kobayashi, *Phys. Rev. B* **58**, 11 169 (1998).
- ²⁷M. Baziljevich, D. Giller, M. McElfresh, Y. Abulafia, Y. Radzyner, J. Schneck, T. H. Johansen, and Y. Yeshurun, *Phys. Rev. B* **62**, 4058 (2000).
- ²⁸Y. Kodama, K. Oka, Y. Yamaguchi, Y. Nishihara, and K. Kajimura, *Phys. Rev. B* **56**, 6265 (1997).
- ²⁹S. B. Roy and P. Chaddah, *Physica C* **279**, 70 (1997).
- ³⁰G. Ravikumar, V. C. Sahni, P. K. Mishra, T. V. Chandrasekhar Rao, S. S. Banerjee, A. K. Grover, S. Ramakrishnan, S. Bhattacharya, M. J. Higgins, E. Yamamoto, Y. Haga, M. Hedo, Y. Inada, and Y. Onuki, *Phys. Rev. B* **57**, R11 069 (1998).
- ³¹R. Cubitt, E. M. Forgan, G. Yang, S. L. Lee, D. Paul, H. A. Mook, M. Yethiraj, P. H. Kes, T. W. Li, A. A. Menovsky, Z. Tarnawski, and K. Mortensen, *Nature (London)* **365**, 407 (1993).
- ³²S. L. Lee, P. Zimmermann, H. Keller, M. Warden, I. M. Savic, R. Schauwecker, D. Zech, R. Cubitt, E. M. Forgan, P. H. Kes, T. W. Li, A. A. Menovsky, and Z. Tarnawski, *Phys. Rev. Lett.* **71**, 3862 (1993).
- ³³A. Schilling, R. A. Fisher, N. E. Phillips, U. Welp, W. K. Kwok, and G. W. Crabtree, *Phys. Rev. Lett.* **78**, 4833 (1997).
- ³⁴J. Kierfeld, *Physica C* **300**, 171 (1998).
- ³⁵T. Nishizaki, T. Naito, S. Okayasu, A. Iwase, and N. Kobayashi, *Phys. Rev. B* **61**, 3649 (2000).
- ³⁶Y. Togawa, T. Sasagawa, J. Shimoyama, and K. Kishio, in *Advances in Superconductivity XI. Proceedings of the 11th International Symposium on Superconductivity, Tokyo, Japan*, edited by N. Koshizuka and S. Tajima (Springer-Verlag, Berlin, 1999), pp. 613–616.
- ³⁷Y. Radzyner, S. B. Roy, D. Giller, Y. Wolfus, A. Shaulov, P. Chaddah, and Y. Yeshurun, *Phys. Rev. B* **61**, 14 362 (2000).
- ³⁸Y. Abulafia, A. Shaulov, Y. Wolfus, R. Prozorov, L. Burlachkov, Y. Yeshurun, D. Majer, E. Zeldov, H. Wuhl, V. B. Geshkenbein, and V. M. Vinokur, *Phys. Rev. Lett.* **77**, 1596 (1996).
- ³⁹A better criterion would be H_{pf} , the height of the profile at a given field. This cannot be measured using global techniques, but can be estimated by the field change needed for a complete reversal of the profile.
- ⁴⁰S. Kokkaliaris, P. A. J. de Groot, S. N. Gordeev, A. A. Zhukov, R. Gagnon, and L. Taillefer, *Phys. Rev. Lett.* **82**, 5116 (1999).
- ⁴¹C. P. Bean, *Phys. Rev. Lett.* **8**, 250 (1962).
- ⁴²D. Giller, A. Shaulov, T. Tamegai, and Y. Yeshurun, *Phys. Rev. Lett.* **84**, 3698 (2000).
- ⁴³Y. Paltiel, E. Zeldov, Y. N. Myasoedov, H. Shtrikman, S. Bhattacharya, M. J. Higgins, Z. L. Xiao, E. Y. Andrei, P. L. Gammel, and D. J. Bishop, *Nature (London)* **403**, 398 (2000).
- ⁴⁴S. B. Roy, P. Chaddah, and S. Chaudhary, *Phys. Rev. B* **62**, 9191 (2000).
- ⁴⁵The absence of history dependence effects in $\text{HgBa}_2\text{CuO}_4$ is also probably related to similar smearing effects of the transition.
- ⁴⁶G. Blatter, V. B. Geshkenbein, and A. I. Larkin, *Phys. Rev. Lett.* **68**, 875 (1992).
- ⁴⁷M. C. de Andrade, N. R. Dilley, F. Ruess, and M. B. Maple, *Phys. Rev. B* **57**, R708 (1998).
- ⁴⁸A. E. Koshelev and V. M. Vinokur, *Phys. Rev. Lett.* **73**, 3580 (1994).
- ⁴⁹Y. Radzyner, A. Shaulov, and Y. Yeshurun, *Phys. Rev. B* **65**, R100 513 (2002).
- ⁵⁰N. Avraham, B. Khaykevich, Y. Myasoedov, M. Rappaport, H. Shtrikman, D. E. Feldman, T. Tamegai, P. H. Kes, L. Ming, M. Konczykowski, K. van der Beek, and E. Zeldov, *Nature (London)* **411**, 451 (2001).
- ⁵¹C. J. van der Beek, S. Colson, M. V. Indenbom, and M. Konczykowski, *Phys. Rev. Lett.* **84**, 4196 (2000).